

MATHEMATICAL MODELLING OF TUBULAR-PLATE LEAD/ACID BATTERIES

O. E. ABDEL-SALAM

Chemical Engineering Department, University of Science & Technology, Irbid (Jordan)

Introduction

Tubular-plate lead/acid batteries are finding increasing application in several market areas, especially in Europe and Japan [1]. The long life, dimensional stability, and reliability all contribute to the success of these batteries in the power industry.

Modelling of lead/acid batteries is an area of active research [2 - 9]. Most of these studies have concentrated on flat-plate batteries. By contrast, little work [2, 9] has been carried out on the modelling of tubular-plate batteries. The early work of Euler and Horn [2] was based on the use of electrical analogs for simulating the current distribution in tubular electrodes. More recently, Lin *et al.* [9] have developed a pseudo steady-state model for the H_2SO_4 concentration, reaction rate, and degree of discharge of tubular positive (PbO_2) electrodes during discharge. The model consists of a set of coupled, non-linear, differential equations that are usually solved numerically [9].

The purpose of the work presented here is to develop a simple, analytical model for the charge/discharge behaviour of the positive PbO_2 tubular electrode. Such a model will facilitate the design and optimization of batteries using tubular-plate electrodes. Theoretical representation of the complete cell is not possible with the present model because the complicated geometrical configuration of tubular-plate types requires the solution of coupled, non-linear, partial differential equations.

Mathematical model

The modelling of a tubular-plate positive PbO_2 electrode gives rise to the following three differential equations [9].

$$\left(\frac{D_c}{D_o}\right) \frac{dC'}{dR'} + (3 - 2t_1) \left(\frac{\epsilon_o}{\epsilon}\right) fi = 0 \quad (1)$$

$$a \left(\frac{\epsilon}{\epsilon_o}\right) \frac{d\eta'}{dR'} = \left(a \frac{dE'}{dC'} - b\right) \left[\left(\frac{D_o}{D_c}\right)(3 - 2t_1)f + 1\right] i - \frac{k_o}{\sigma_c} \quad (2)$$

$$\frac{di}{dR'} = h \left(1 - \frac{X}{X_{max}}\right) \exp(-2\eta') - \frac{i}{R'} \quad (3)$$

where: D is the diffusion coefficient of the acid (the subscripts c and o represent the values in the cathode and free solution, respectively); C' is the ratio between C , the concentration at radius r , and C_o ; R' is the ratio between r and L which is the outer radius of the electrode; t_1 is the transference number of H^+ ions; ε is the porosity; f is a factor equal to $IL/2FD_oC_o$ where I is the total current density; i is the ratio between i_2 (the current density in the electrolyte) and I ; a is equal to (k_oRT/FLI) where k is the conductivity of the electrolyte; η' is equal to $F\eta/RT$ where η is the overpotential; E' is equal to (FE_{eq}/RT) ; b is equal to $(F(D_1 - D_2)C_o/IL)$ where the subscripts 1 and 2 represent H^+ and HSO_4^- , respectively; σ is the conductivity of the electrode material; h is equal to $-LS_o i_o/I$ where S_o is the initially available active surface in a fully charged electrode and i_o is the exchange current density; X is the degree of discharge; X_{max} is the maximum fraction of the electrode material that can be utilized at a given current density.

The porosity, ε , is related to X as follows:

$$\varepsilon = \varepsilon_o - g(1 - \varepsilon_o)X \quad (4)$$

where g is a constant and has a value of 0.917.

The degree of discharge (DOD) is dependent upon the current according to:

$$X = -\frac{IL}{D_o q_o} \int_0^{\tau} \frac{1}{R'} \frac{d(R'i)}{dR'} d\tau \quad (5)$$

where q_o is the quantity of the charge available initially per unit volume.

The boundary conditions for eqns. (4) and (5) are:

$$R' = 0, \quad i = \frac{dC'}{dR'} = 0$$

$$R' = 1, \quad i = C' = 1$$

Instead of solving these equations numerically, as was the procedure in ref. 9, it will be assumed that C is given by the following expression:

$$C = \frac{m + R'^2}{m + 1} \quad (6)$$

This relationship fits the above boundary conditions and closely matches the numerical solution [9]. Substitution of eqns. (4) and (6) in eqn. (1) gives the following linear differential equation:

$$\frac{di}{dR'} + \frac{N}{R'} i = -\frac{1}{K} \quad (7)$$

where N is equal to:

$$1 + \frac{(3 - 2t_1)D_o \varepsilon_o q_o}{2FD_c C_o g(1 - \varepsilon_o)\tau} (m + 1)$$

and K is equal to:

$$g\left(\frac{1-\varepsilon_0}{\varepsilon_0}\right) \frac{IL\tau}{D_0q_0}$$

The solution of eqn. (7) with the boundary condition of $i = 1$ at $R' = 1$ is:

$$i = \left(1 + \frac{1}{K(N+1)}\right) \frac{1}{(R')^N} - \frac{1}{K(N+1)} R' \quad (8)$$

and on substitution in eqn. (5) yields:

$$X = -P \left[(1-N) \left(1 + \frac{1}{K(N+1)}\right) R'^{-(N+1)} - \frac{2}{K(N+1)} \right] \quad (9)$$

where P is equal to $IL\tau/D_0q_0$.

Finally, the overpotential can be obtained by substitution into eqn. (3) as follows:

$$\eta' = -\frac{1}{2} \ln \frac{-X/P}{h(1-X/X_{\max})} \quad (10)$$

The solution given by eqn. (9) at $R' = 0$ fails. Instead, if eqn. (7) is first taken, and with the knowledge that

$$\lim_{R' \rightarrow 0} \frac{i}{R'} = \frac{di}{dR'} \quad (11)$$

then, X at $R' = 0$ is given by the following:

$$X = \frac{2P}{K(N+1)} \quad (12)$$

The value of m can be obtained by substitution of eqns. (6), (8) and (10) in eqn. (2) and by employing a least-square fitting as follows:

$$\frac{d}{dm} \left(\int_0^1 G^2(m, R') dR' \right) = 0 \quad (13)$$

where G is the difference between the left-hand and right-hand sides of eqn. (2). The value of m can be calculated either by means of a numerical method (e.g., the Newton-Raphson method) or by a graphical approach (see Appendix A).

During battery charging, eqns. (1) and (2) are valid whereas eqn. (3) is replaced by the following relationship due to the depletion of PbSO_4 as PbO_2 is being formed [8]:

$$\frac{di}{dR'} = h \left(1 - \frac{1}{X_{\max}}\right) \frac{X}{X_{\max}} \exp(-2\eta') - \frac{i}{R'} \quad (14)$$

Results

Although there were no data available for concentration, reaction rate, rate of discharge, and potential distributions in tubular-plate cells, the model was used to determine these in a number of cases. In particular, the effects of current density, electrode thickness, time of discharge and concentration were studied.

Effect of current density

The model was used to calculate the H_2SO_4 concentration, current density, degree of discharge, and overpotential distributions for an electrode radius of 0.1 cm, an H_2SO_4 concentration of $4.9 \times 10^{-3} \text{ mol cm}^{-3}$, a discharge time of 90 min, and current densities of 25 and 100 A m^{-2} . The results are shown in Figs. 1 - 4.

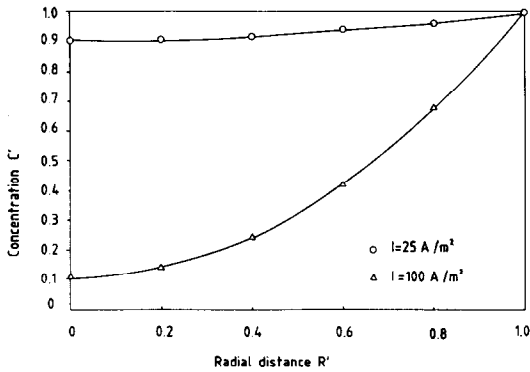


Fig. 1. Concentration distribution at 25 and 100 A m^{-2} . Time = 90 min; electrode radius = 0.1 cm; H_2SO_4 concentration = $4.9 \times 10^{-3} \text{ mol cm}^{-3}$.

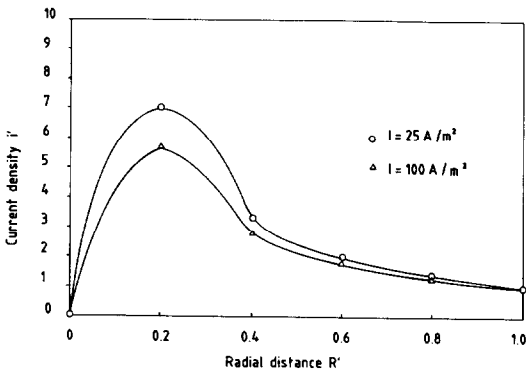


Fig. 2. Local current-density distribution at 25 and 100 A m^{-2} . Time = 90 min; electrode radius = 0.1 cm; H_2SO_4 concentration = $4.9 \times 10^{-3} \text{ mol cm}^{-3}$.

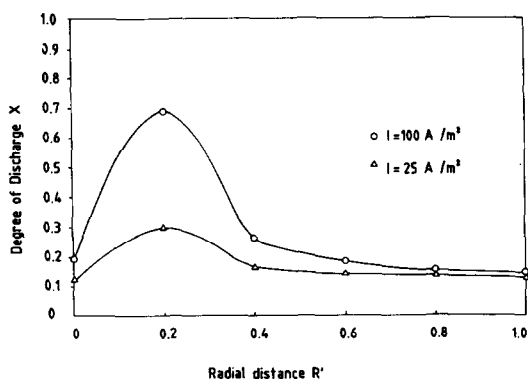


Fig. 3. Degree of discharge distribution at 25 and 100 A m⁻². Time = 90 min; electrode radius = 0.1 cm; H₂SO₄ concentration = 4.9 × 10⁻³ mol cm⁻³.

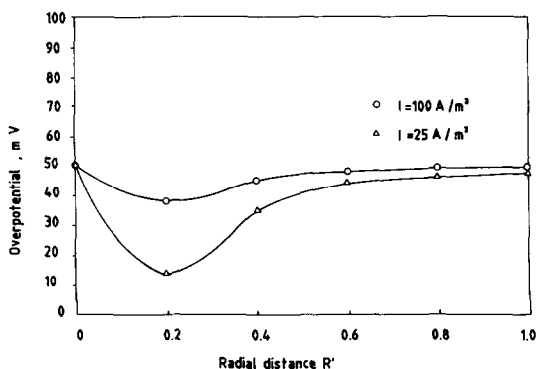


Fig. 4. Overpotential distribution at 25 and 100 A m⁻². Time = 90 min; electrode radius = 0.1 cm; H₂SO₄ concentration = 4.9 × 10⁻³ mol cm⁻³.

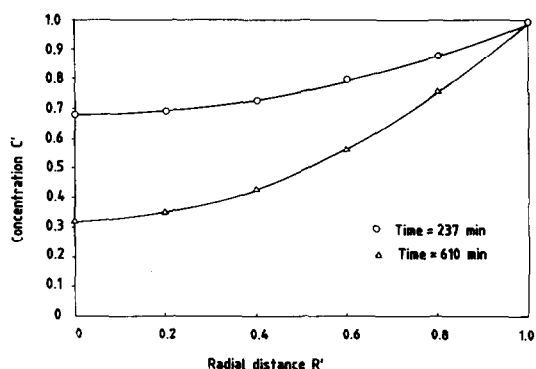


Fig. 5. H₂SO₄ concentration distribution at 237 and 610 min. Current density = 25 A m⁻²; electrode radius = 0.3 cm; H₂SO₄ concentration = 4.9 × 10⁻³ mol cm⁻³.

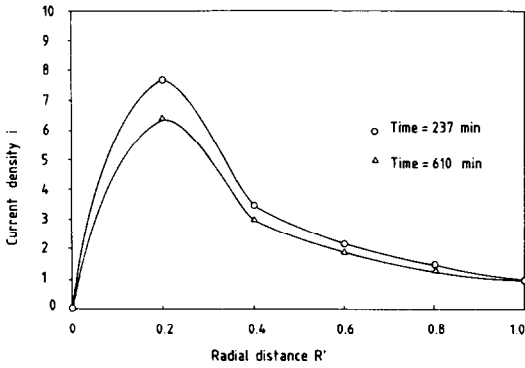


Fig. 6. Local current-density distribution at 237 and 610 min. Current density = 25 A m^{-2} ; electrode radius = 0.3 cm ; H_2SO_4 concentration = $4.9 \times 10^{-3} \text{ mol cm}^{-3}$.

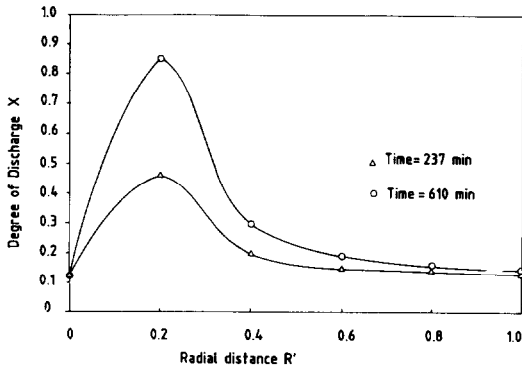


Fig. 7. Degree of discharge distribution at 237 and 610 min. Current density = 25 A m^{-2} ; electrode radius = 0.3 cm ; H_2SO_4 concentration = $4.9 \times 10^{-3} \text{ mol cm}^{-3}$.

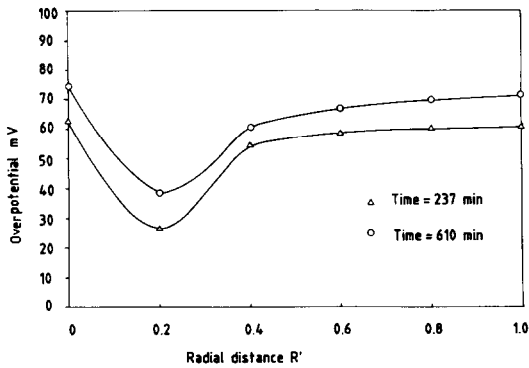


Fig. 8. Overpotential distribution at 237 and 610 min. Current density = 25 A m^{-2} , electrode radius = 0.3 cm ; H_2SO_4 concentration = $4.9 \times 10^{-3} \text{ mol cm}^{-3}$.

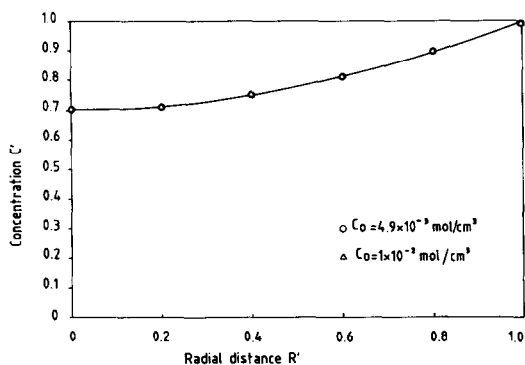


Fig. 9. H₂SO₄ concentration distribution at 4.9×10^{-3} and 1×10^{-2} mol cm⁻³. Current density = 50 A m^{-2} ; time = 255 min; electrode radius = 0.1 cm.

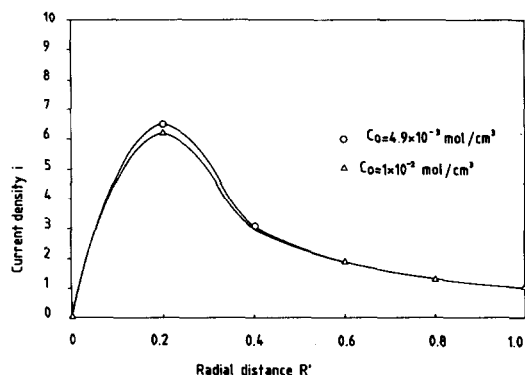


Fig. 10. Local current-density distribution at 4.9×10^{-3} and 1×10^{-2} mol cm⁻³ H₂SO₄. Current density = 50 A m^{-2} ; time = 255 min; electrode radius = 0.1 cm.

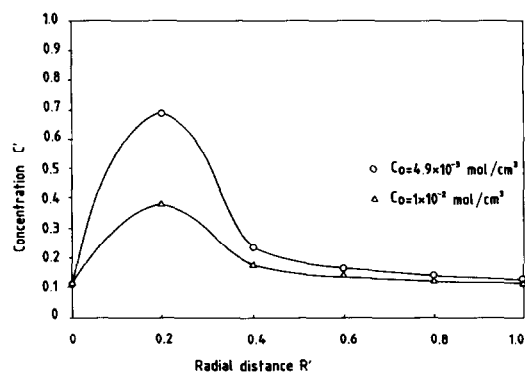


Fig. 11. Degree of discharge distribution at 4.9×10^{-3} and 1×10^{-2} mol cm⁻³ H₂SO₄. Current density = 50 A m^{-2} ; time = 255 min; electrode radius = 0.1 cm.

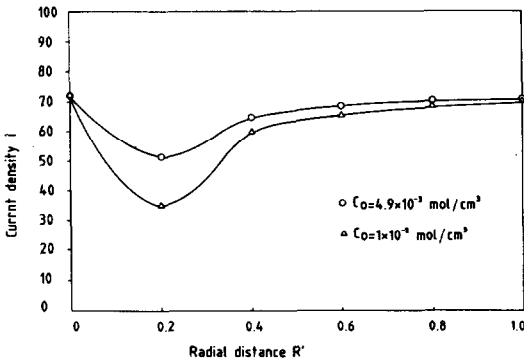


Fig. 12. Overpotential distribution at 4.9×10^{-3} and $1 \times 10^{-2} \text{ mol cm}^{-3} \text{ H}_2\text{SO}_4$. Current density = 50 A m^{-2} ; time = 255 min; electrode radius = 0.1 cm.

The data show that as the current density increases, the concentration decrease becomes more steep. The local current density increases to a maximum at around $R = 0.2$ and then decreases to its lowest value at the outer radius. The degree of discharge shows a similar pattern as it is directly dependent on the current density. The overpotential increases with total current density.

Effect of discharge time

An increase in the charging time results in a larger drop in electrolyte concentration, a larger degree of discharge, a lower current density and a higher overpotential. These findings are evident from the results shown in Figs. 5 - 8 and are consistent with the effect of discharge time on these parameters.

Effect of electrode radius

The effect of electrode radius can be examined by comparison of the curves in Figs. 5 - 8, with Figs. 9 - 12 that are plotted for a radius of 0.3 cm and 0.1 cm, respectively. The results show that the degree of discharge increases as the electrode radius decreases.

Effect of electrolyte concentration

The effect of increasing the H_2SO_4 concentration from 4.9×10^{-3} to $1 \times 10^{-2} \text{ mol cm}^{-3}$ is shown in Figs. 9 - 12. The data reveal that both the degree of discharge and the overpotential decrease with increase in electrolyte concentration.

Conclusions

It is possible with the present model to simulate the behaviour of the positive electrode of lead/acid batteries under different conditions of current

density, discharge time, electrode radius, and electrolyte concentration. Although the determination of actual current distributions by the analysis of reaction products is rather tedious [10], the model can be tested in the future when enough data are available for comparison.

Acknowledgements

The author is grateful to M. Al Shobaki and H. Al-Taani for assistance with the calculations.

References

- 1 H. Miura, *J. Power Sources*, **32** (1988) 93.
- 2 J. Euler and L. Horn, *Electrochim. Acta*, **10** (1965) 1057.
- 3 D. Simonsson, *J. Appl. Electrochem.*, **3** (1973) 261.
- 4 D. Simonsson, *J. Appl. Electrochem.*, **4** (1974) 109.
- 5 K. Micka and I. Rousar, *Electrochim. Acta*, **18** (1973) 629.
- 6 W. H. Tiedemann and J. Newman, in S. Gross (ed.), *Battery Design and Optimisation*, The Electrochemical Society, Princeton, NJ, 1979, p. 23.
- 7 W. S. Sunu, in R. E. White (ed.), *Electrochemical Cell Design*, Plenum Press, New York, 1984, p. 357.
- 8 H. Gu, T. V. Nguyen and R. E. White, *J. Electrochem. Soc.*, **134** (1987) 2953.
- 9 K. M. Lin, Y. Y. Wang and C. C. Wan, *J. Appl. Electrochem.*, **18** (1988) 590.
- 10 D. Simonsson, *J. Electrochem. Soc.*, **120** (1973) 151.

Appendix A

Sample calculation of m

For a current density of 25 A m^{-2} , a time of 610 min, an electrode radius of 0.3 cm, and an H_2SO_4 concentration of $4.9 \times 10^{-3} \text{ mol cm}^{-3}$, the expressions of C , i , X and η were substituted in eqn. (2) and the difference between the left-hand and right-hand sides was used to calculate the integral $(\int_0^1 G^2(m, R') dR')$. This integral was plotted as a function of m in Fig. 13. The minimum was found to be at $m = 0.47$. This value of m was subsequently used to obtain the concentration, reaction rate, state-of-discharge and overpotential distributions shown in Figs. 5 - 8, respectively.

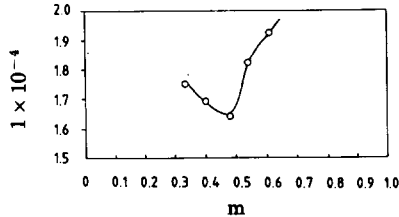


Fig. 13. Graphical determination of m .